Bioorganic Chemistry 38 (2010) 165–172

Contents lists available at ScienceDirect

Bioorganic Chemistry

journal homepage: www.elsevier.com/locate/bioorg

# The effective molarity (EM) – A computational approach

Rafik Karaman *

*Faculty of Pharmacy, Al-Quds University, P.O. Box 20002, Jerusalem, Palestine*

ARTICLE INFO

*Article history:*
Received 19 February 2010
Available online 10 April 2010

*Keywords:*
Effective molarity (EM)
$S_N2$ ring-closing reactions
MP2 and DFT calculations
Proximity orientation
Steric effects

ABSTRACT

The effective molarity (EM) for 12 intramolecular $S_N2$ processes involving the formation of substituted aziridines and substituted epoxides were computed using *ab initio* and DFT calculation methods. Strong correlation was found between the calculated effective molarity and the experimentally determined values. This result could open a door for obtaining EM values for intramolecular processes that are difficult to be experimentally provided. Furthermore, the calculation results reveal that the driving forces for ring-closing reactions in the two different systems are proximity orientation of the nucleophile to the electrophile and the ground strain energies of the products and the reactants.



## 1. Introduction

Intramolecular processes proceed faster than their intermolecular counterparts due simply to the way of the reactive centers are brought together. The similarity in the orientation of the reactive centers in enzymes and intramolecular processes (covalently with intramolecular systems, and non-covalently with enzymes) inspired many chemists to utilize intramolecularity to better understand the mechanism(s) by which enzymes exert their high catalytic efficiency [1].

Since 1960 reaction models for mimicking enzyme catalysis has been advocated by a variety of bioorganic chemists. Among enzyme models based on enthalpic driving forces are: (i) "near attack proximity orientation" model proposed by Bruice's group [2]; (ii) "orbital steering theory" proposed by Koshland's group [3]; (iii) "spatiotemporal hypothesis" devised by Menger et al. [4]; and (iv) "stereopopulation control" suggested by Cohen's group [5]. On the other hand, Jencks and Page have proposed that the origin of rate accelerations of intramolecular processes is due to entropic effects such that the loss of translational and rotational entropy slows intermolecular reactions but not intramolecular reactions [6].

Mechanistic studies based on these models have played an important role in elucidating the chemistry of the groups involved in enzyme catalysis as well as in unraveling the mechanisms available for particular processes. Based on these studies it seems reasonable to assume that an understanding how efficiency depends on structure in intramolecular catalysis well shed some light on the related problems in enzyme catalysis.

One measure commonly used for intramolecular efficiency is the effective molarity parameter (EM). EM is defined as $k_{intra}/k_{inter}$ for corresponding intramolecular and intermolecular processes driven by identical mechanisms. Kirby's report of EM values indicates that they can range from less than 0.3 M up to more than $10^{16}$ M. The factors affecting the value of EM are ring size, solvent and reaction type [7]. Accurate measurements of EM values have stringent requirements: (a) the mechanisms of both intramolecular and the corresponding intermolecular processes must be the same. (b) Rate measurements for both reactions should be carried under the same conditions. The difficulty in achieving these two stringent requirements resulted in the availability of effective molarities for only a handful of reactions. Hence there is a pressing need to find alternative ways for obtaining EM values for certain important intramolecular processes that ordinary methods were failed to provide.

Recently, we have been extensively engaged in exploring the origin of the driving forces for the extraordinary enhancements in rate of a significant number of intramolecular processes [8]. Exploiting the *ab initio* and the DFT molecular orbital methods we computed the mechanistic behavior for acid-catalyzed lactonization of hydroxy-acids as studied by Cohen and coworkers [5] and Menger and coworkers [4], cyclization reactions of di-carboxylic semi esters to yield anhydrides as studied by Bruice and coworkers [2], intramolecular proton-transfers in rigid systems as studied by Menger and coworkers [4] and $S_N2$-based ring-closing reactions as studied by Mandolini's group [9]. The main conclusions that emerged from these studies suggest: (1) both, strain and unstrained proximity effects play important role in determining the closeness of an electrophile to a nucleophile and consequently enhancing or inhibiting the reaction rate. (2) The nature of the reaction being intermolecular or intramolecular is determined on

* Fax: +972 22790413
*E-mail address:* dr_karaman@yahoo.com

0045-2068/$ - see front matter © 2010 Elsevier Inc. All rights reserved.
doi:10.1016/j.bioorg.2010.04.002

the distance between a nucleophile and an electrophile. (3) In $S_N2$-based ring-closing reactions leading to three-, four- and five-membered rings the *gem*-dialkyl effect is more dominant in the processes involving the formation of an unstrained five-membered ring and the need for directional flexibility decreases with the increasing size of the ring being formed. In addition, the demands on directional flexibility decrease with the increase in the volume of the nucleophile involved in the $S_N2$ ring-closing reaction. (4) Enthalpic as well as entropic effects are both important factors in enhancing the rate of the intramolecular process. This is contrary to Bruice's proposal that indicates enthalpic effects are the main driving force for such accelerations [2].

In this manuscript, we describe our DFT and *ab initio* MP2 quantum molecular orbital investigations of transition state structures, vibrational frequencies, and reaction trajectories for ring-closing reactions of substituted 3-aminoalkyl halides and substituted chlorohydrins to substituted aziridines and substituted epoxides, respectively. The activation energies for these processes as well as for that of the corresponding intermolecular processes were used in the calculations of the effective molarities.

We have chosen to study these two systems because: (a) the experimental effective molarity obtained for the two systems were based on accurate measurements of the rate constant for the intramolecular reaction and the rate constant for the closest equivalent intermolecular reaction under conditions which are as similar as possible. This allows us to make precise and justified comparisons of the calculated EM values with that experimentally determined. (b) Intramolecular processes leading to substituted aziridines and substituted epoxides have been known for very long time but till now there is no experimental or theoretical sharp evidence on the nature of the driving forces responsible for the high rate accelerations in these systems.

## 2. Calculation methods

The *ab initio* and DFT calculations were carried out using the quantum chemical package Gaussian-98 [10]. The MM2 molecular mechanics strain energy calculations were performed using Allinger's MM2 program installed in Chem 3D Ultra 8.0 [11]. The starting geometries of all the molecules presented in this study were obtained using the Argus Lab program [12] and were initially optimized at the AM1 level of theory [10]. The calculations were carried out based on the restricted Hartree–Fock (RHF) method with full optimization of all geometrical variables [13]. The global minimum structures of the starting materials were found by conducting rotations of 360° around the C2–C3 bond where applicable. To avoid results with local minima optimization, frequency calculation were carried out. An energy minimum (a stable compound or a reactive intermediate) has no negative vibrational force constant. A transition state is a saddle point which has only one negative vibrational force constant [14]. The "reaction coordinate method" was used to calculate the activation energy in systems **1**–**12** [15]. In this method, one bond length is constrained for the appropriate degree of freedom while all other variables are freely optimized. The activation energy values for ring-closing reactions of **1**–**12** were calculated from the difference in energies of the global minimum structures (GM) and the derived transition states (TS). Verification of the desired reactants and products was accomplished using the "intrinsic coordinate method" [15]. The transition state structures were verified by their only one negative frequency. Full optimization of the transition states was accomplished after removing any constrains imposed while executing the energy profile. The activation energies obtained from the DFT and the MP2 for **1**–**12** were calculated with and without the inclusion of solvent (water). The calculations with the incorporation of a solvent were performed using the integral equation formalism model of the Polarizable Continuum Model (PCM) [16].

## 3. Results and discussion

Using the quantum chemical package Gaussian-98 [10] we have calculated the DFT B3LYP/6-31G (*d*, *p*) kinetic and thermodynamic parameters for the intramolecular processes **1**–**6** and **7**–**12** (Chart 1) and their corresponding intermolecular processes **13**–**15** and **16**–**18**, respectively (Chart 2). The intermolecular processes **13**–**15** and **16**–**18** were chosen since theses processes were originally utilized in the experimental studies for the determination of the EM values for the corresponding intramolecular processes **1**–**12**. For intramolecular processes **7**–**12** and their corresponding intermolecular reactions, **16**–**18**, *ab initio* MP2 calculations were carried out as well.

The calculated MP2 and DFT enthalpic and entropic energies for the global minimum (GM) and transition state structures (TS) for **1**–**12** along with their corresponding intermolecular processes are summarized in Table 1. Figs. 1a and 1b illustrate the calculated *ab initio* and DFT optimized global minimum (GM) and transition state (TS) structures for processes **1**, **6**, **7** and **10**. Examination of the TS optimized structures for **1**–**12** (Figs. 1a and 1b) indicates that in processes leading to substituted aziridines (**1**–**6**) the transition state is reached when the distance between the amine nitrogen (N1) and the carbon attached to Cl (C2) is about 1.82 Å, whereas for the processes leading to substituted epoxides (**7**–**12**) the transition state is achieved when the distance is between 2.1 Å and 2.2 Å. This suggests an early transition state for processes yielding to epoxide rings and a relatively late transition state for intramolecular ring-closing reactions providing aziridine rings. Inspection of Figs. 1a and 1b reveals that the gas phase calculated global optimum and transition state structures in both **1**–**6** and **7**–**12** derivatives have similar conformational pattern such that the nucleophile (N1 in **1**–**6** and $O1^-$ in **7**–**12**), the carbon attached to chloride (C2) and chlorine (Cl4) in a co linearity complying with Baldwin rules. It should be noted that the same picture was obtained when the same calculations were carried out in the presence of one molecule of water.

Using the calculated enthalpies and entropies for the GM and TS structures in **1**–**12** (Table 1), we have calculated the enthalpic activation energies ($\Delta H^{\ddagger}$), entropic activation energies ($T\Delta S^{\ddagger}$), and free activation energies in the gas phase ($\Delta G^{\ddagger}$) and in water and ether ($\Delta G_s^{\ddagger}$) (Chart 1) for the corresponding intramolecular ring-closing reactions. The calculated DFT and *ab initio* MP2 values are summarized in Table 2. Also included in the table are the MM2 strain energies for the reactants and the products ($\Delta E_s$) and the experimental log EM and log $k_{rel}$ values.

In order to calculate the EM values for processes **1**–**12** we have calculated the DFT and MP2 activation free energies ($\Delta G_S^{\ddagger}$) for the corresponding intermolecular processes **13**–**15** and **16**–**18**, where **13**–**15** are the corresponding intermolecular processes for **1**–**6** and **16**–**18** are for that of **7**–**12** (Chart 2).

Using Eqs. (1)–(4), we have derived Eq. (5) that describes the EM term as a function of the difference in the activation energies of the intra- and the corresponding intermolecular processes. The values calculated by Eq. (5) for processes **1**–**12** in different media are listed in Table 2.

$$EM = k_{\text{intra}}/k_{\text{inter}} \tag{1}$$

$$\Delta G_{S\ \text{inter}}^{\ddagger} = -RT\ln k_{\text{inter}} \tag{2}$$

$$\Delta G_{S\ \text{intra}}^{\ddagger} = -RT\ln k_{\text{intra}} \tag{3}$$

$$\Delta G_{S\ \text{intra}}^{\ddagger} - \Delta G_{\text{inter}}^{\ddagger} = -RT\ln k_{\text{intra}}/k_{\text{inter}} \tag{4}$$

$$\ln EM = -(\Delta G_{S\ \text{intra}}^{\ddagger} - \Delta G_{S\ \text{inter}}^{\ddagger})/RT \tag{5}$$

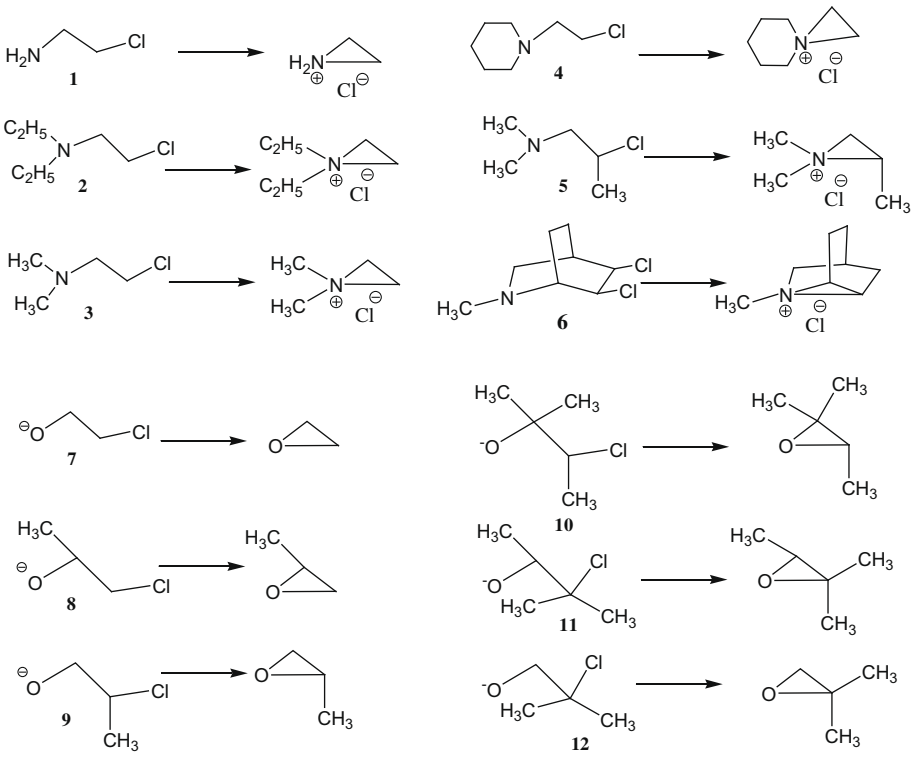

**Chart 1.** Intramolecular ring-closing reaction for processes **1**–**12**.

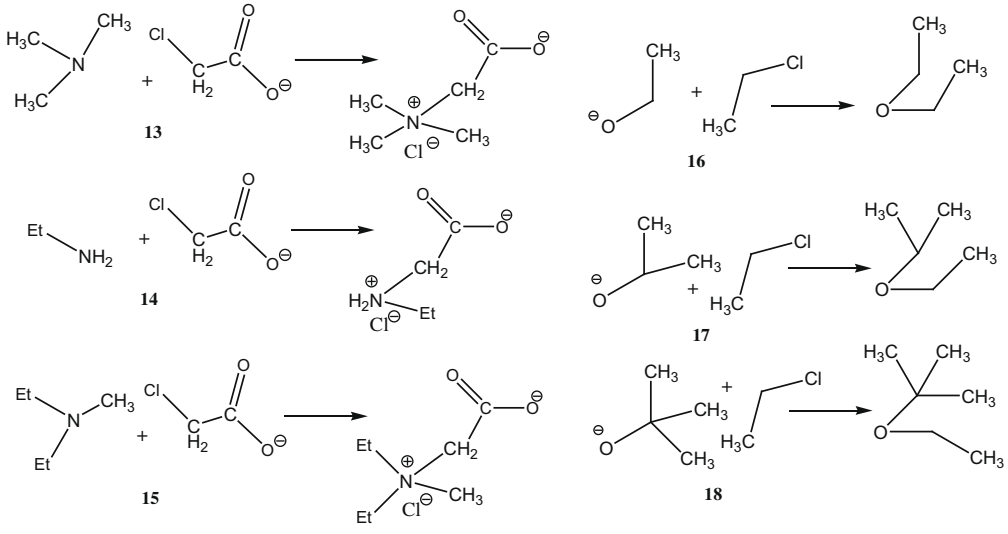

**Chart 2.** Intermolecular $S_N2$ reaction for processes **13**–**18**.

where $T$ is a temperature in K and $R$ is the gas constant.

### 3.1. Ring-closing reactions of substituted 3-aminoalkyl halides

The calculated DFT effective molarities for processes **1**–**6** that are listed in Table 2 were examined for linear correlation with the experimentally determined values. The correlation results along with the correlation coefficients ($R$) are summarized in Eqs. (6)–(8) and are graphically illustrated in Fig. 2a, where Eqs. (6)–(8) represent the correlation of the experimental data with that calculated in the gas phase, ether and water, respectively.

$$\log EM(\text{calc}) = 1.797 \log EM(\text{exp}) + 2.483 \quad (R = 0.98) \tag{6}$$

$$\log EM(\text{calc}) = 1.850 \log EM(\text{exp}) - 2.383 \quad (R = 0.93) \tag{7}$$

$$\log EM(\text{calc}) = 1.886 \log EM(\text{exp}) - 4.919 \quad (R = 0.95) \tag{8}$$

Careful examination of the equations and the figure reveals the following: (i) strong correlation exists between the calculated and the experimental EM values. (ii) The type of the reaction solvent has a profound effect on the EM values. In solvents with high dielectric constants such as water the ratio $k_{intra}/k_{inter}$ is much lower than that in the gas phase or in solvents having low dielectric constant values. This is because in solvents having high dielectric constants, such as water, the intermolecular transition state

**Table 1**
HF, MP2 and DFT calculated properties for the reactions of **1–18**.

| Compound | HF enthalpy, *H* (gas phase) in Hartree | HF (gas phase) (entropy, *S*, Cal/Mol-K | HF frequency $cm^{-1}$ | B3LYP enthalpy, *H* (gas phase) in Hartree | B3LYP (gas phase) entropy, *S*, Cal/Mol-K | B3LYP frequency $cm^{-1}$ |
|---|---|---|---|---|---|---|
| 1GM | −593.0767729 | 74.62 | | −594.7730161 | 72.98 | |
| 1TS | −593.0222894 | 71.86 | 536.49i | −594.7221635 | 76.98 | 325.14i |
| 2GM | −749.1304822 | 98.52 | | −752.0306604 | 100.57 | |
| 2TS | −749.0783501 | 96.31 | 542.12i | −751.9766836 | 97.01 | 389.08i |
| 3GM | −671.0918945 | 87.16 | | −673.3964341 | 86.94 | |
| 3TS | −671.0435277 | 84.64 | 546.55i | −673.3452548 | 84.78 | 357.39i |
| 4GM | −786.9904727 | 96.91 | | −790.1404723 | 96.15 | |
| 4TS | −786.9447387 | 92.94 | 543.17i | −790.0921205 | 94.18 | 376.51i |
| 5GM | −710.1154475 | 92.88 | | −712.7169671 | 93.19 | |
| 5TS | −710.0656223 | 92.73 | 442.20i | −712.6602798 | 91.31 | 400.68i |
| 6GM | −1283.7157873 | 97.83 | | −1287.8299983 | 99.22 | |
| 6TS | −1283.6657461 | 99.98 | 371.57i | −1287.7794472 | 99.70 | 347.39i |
| 7GM | −612.3632479 [a] | 70.38 [a] | | −614.0517701 [b] | 72.19 [b] | |
| 7TS | −612.3575619 [a] | 69.53 [a] | 335.66i [a] | −614.0512486 [b] | 70.47 [b] | 180.06i [b] |
| 8GM | −651.4077042 [a] | 76.91 [a] | | −653.3756144 [b] | 79.34 [b] | |
| 8TS | −651.4044711 [a] | 75.75 [a] | 92.74i [a] | −653.3754646 [b] | 77.08 [b] | 61.46i [b] |
| 9GM | −651.4062264 [a] | 76.12 [a] | | −653.3721813 [b] | 77.68 [b] | |
| 9TS | −651.3998037 [a] | 75.73 [a] | 191.42i [a] | −653.3701551 [b] | 77.28 [b] | 191.58i [b] |
| 10GM | −730.5384099 [a] | 94.66 [a] | | −732.0124472 [b] | 91.53 [b] | |
| 10TS | −730.5338181 | 94.13 [a] | 169.39i [a] | −732.0120531 [b] | 90.54 [b] | 195.49i [b] |
| 11GM | −730.5390415 [a] | 94.65 [a] | | −732.0110049 [b] | 89.84 [b] | |
| 11TS | −730.5300183 [a] | 94.15 [a] | 222.31i [a] | −732.0085331 [b] | 90.03 [b] | 192.35i [b] |
| 12GM | −691.3506254 [a] | 75.70 [a] | | −692.6916609 [b] | 82.83 [b] | |
| 12TS | −691.3431931 [a] | 75.80 [a] | 216.12i [a] | −692.6878901 [b] | 83.57 [b] | 198.15i [b] |
| 13GM | – | – | – | −862.61321311 | 118.55 | |
| 13TS | – | – | – | −862.56277291 | 101.02 | 349.02i |
| 14GM | – | – | – | −823.31692951 | 106.82 | |
| 14TS | – | – | – | −823.26532312 | 101.02 | 377.57i |
| 15GM | – | – | – | −941.24826892 | 127.37 | |
| 15TS | – | – | – | −941.19257589 | 111.83 | 360.17i |
| 16GM | – | – | – | −770.33355011 | 112.34 | |
| 16TS | – | – | – | −770.32624782 | 110.92 | 770.33i |
| 17GM | – | – | – | −809.65316192 | 126.11 | |
| 17TS | – | – | – | −809.64716213 | 115.72 | 377.13i |
| 18GM | – | – | – | −848.97676601 | 129.16 | |
| 18TS | – | – | – | −848.96618972 | 116.98 | 344.51i |

HF, MP2 and B3LYP refer to calculated by HF/6-31G, MP2/6-31G and B3LYP/6-31G (*d*, *p*), respectively. GM and TS are global minimum and transition state structures, respectively.
[a] Calculated by MP2.
[b] Calculated by B3LYP/cc-pVDZ.

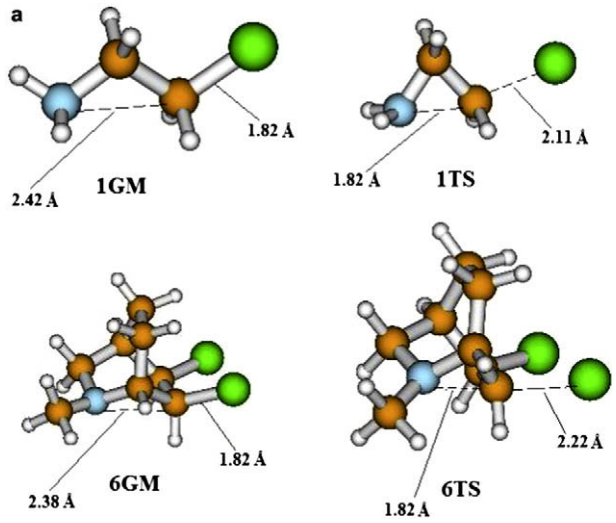


**Fig. 1a.** DFT global minimum and transition state structures for **1**GM, **6**GM, **1**TS and **6** TS.

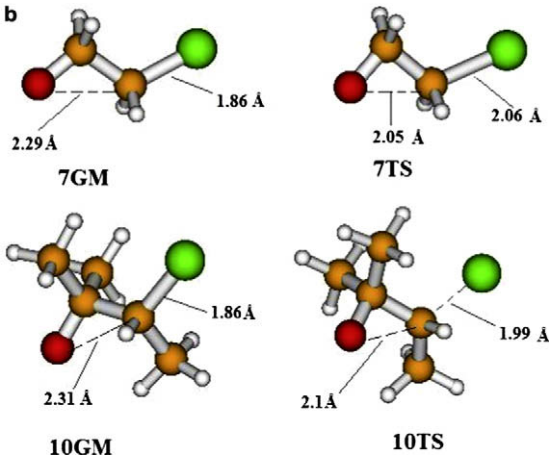


**Fig. 1b.** MP2 optimized structures for **7**GM, **10**GM, **7**TS and **10**TS.

structure is much more stabilized than the corresponding ground state structure. For example, the difference in the enthalpic energy values of the ground state structure for process 13 as calculated in water and in the gas phase is 0.081 Hartree, whereas that calculated for the transition state is 0.112 Hartree. This is might be due to the fact that the intermolecular control system is negatively charged and it is expected that the charge distribution in its transition state will be much more efficient in the presence of the

**Table 2**
DFT and *ab initio* calculated kinetic and thermodynamic properties for the ring-closing reactions of **1**–**12**.

| System | log EM | log $k_{rel}$ | MM2 $\Delta E_s$[a] | GP $\Delta G^{\ddagger}_{inter}$ | GP $\Delta G^{\ddagger}_{intra}$ | GP $\Delta G^{\ddagger}_{inter}$ $\Delta G^{\ddagger}_{intra}$ | $H_2O$ $\Delta G^{\ddagger}_{S\ inter}$ | $H_2O$ $\Delta G^{\ddagger}_{S\ intra}$ | $H_2O$ $\Delta G^{\ddagger}_{S\ inter}$ $\Delta G^{\ddagger}_{S\ intra}$ | Ether $\Delta G^{\ddagger}_{S\ intra}$ | Ether $\Delta G^{\ddagger}_{S\ intra}$ | DFT and MP2 calc (Water) log EM | DFT calc (GP) log EM | DFT calc (Ether) log EM |
|---|---|---|---|---|---|---|---|---|---|---|---|---|---|---|
| 1 | 0 | 0 | 112.72 | 35.60 | 33.36 | 2.24 | 16.31 | 24.57 | −8.26 | 22.39 | 27.78 | −6.0596 | 1.6433 | −3.9541 |
| 2 | 3.3010 | 1.7293 | – | – | – | – | – | – | – | – | – | – | – | |
| 3 | 0.1139 | 1.2188 | 111.22 | 36.87 | 32.70 | 4.17 | 18.62 | 25.18 | −6.56 | 25.70 | 28.24 | −4.8125 | 3.0591 | −1.8633 |
| 4 | 0.7782 | 3.6570 | 110.76 | 36.87 | 30.94 | 5.93 | 18.62 | 21.99 | −3.37 | 25.70 | 25.54 | −2.4722 | 4.3503 | 0.1173 |
| 5 | 0.9542 | 2.9690 | 112.18 | 36.87 | 30.93 | 5.94 | 18.62 | 21.96 | −3.34 | 25.70 | 25.70 | −2.4501 | 4.3576 | 0 |
| 6 | 3.4771 | 6.4409 | 96.99 | 39.35 | 27.90 | 11.68 | 20.82 | 22.51 | 1.69 | 31.59 | 26.64 | 1.2397 | 8.5685 | 3.6314 |
| 7 | 3.3979 | 0 | 8.94 | – | – | – | 10.70 | 9.54 | 1.14 | – | – | 0.8363 | – | – |
| 8 | 5.9030 | 2.2320 | 9.69 | – | – | – | 12.01 | 6.63 | 5.38 | – | – | 3.9468 | – | – |
| 9 | 4.3010 | 0.6530 | 9.69 | – | – | – | 10.70 | 8.48 | 2.22 | – | – | 1.6286 | – | – |
| 10 | 8.9030 | 5.2420 | 12.69 | – | – | – | 14.79 | 5.99 | 8.80 | – | – | 6.4557 | – | – |
| 11 | 8 | 4.4222 | 12.69 | – | – | – | 12.01 | 5.70 | 6.31 | – | – | 4.6291 | – | – |
| 12 | 6 | 2.3104 | 9.61 | – | – | – | 10.70 | 6.93 | 3.77 | – | – | 2.7657 | – | – |

MM2 refer to calculated by Allinger's MM2 methods. log EM is the logarithm of the effective molarity and its values are taken from Ref. [7]. log $k_{rel}$ is the logarithm of the relative rate and its values are taken from Ref. [7]. $\Delta G^{\ddagger}_{intra}$ is the activation energy for the intramolecular process and $\Delta G^{\ddagger}_{inter}$ is the activation energy of the corresponding intermolecular process $\Delta E_s$ is the MM2 difference in strain energies of the products and the reactants in kcal/mol. GP refers to calculated in the gas phase. $H_2O$ refers to calculated in the presence of water as a solvent. Ether refers to calculated in the presence of ether as a solvent.

[a] For systems **7**–**12** the $E_s$ values belong are the MM2 strain energies of the products.

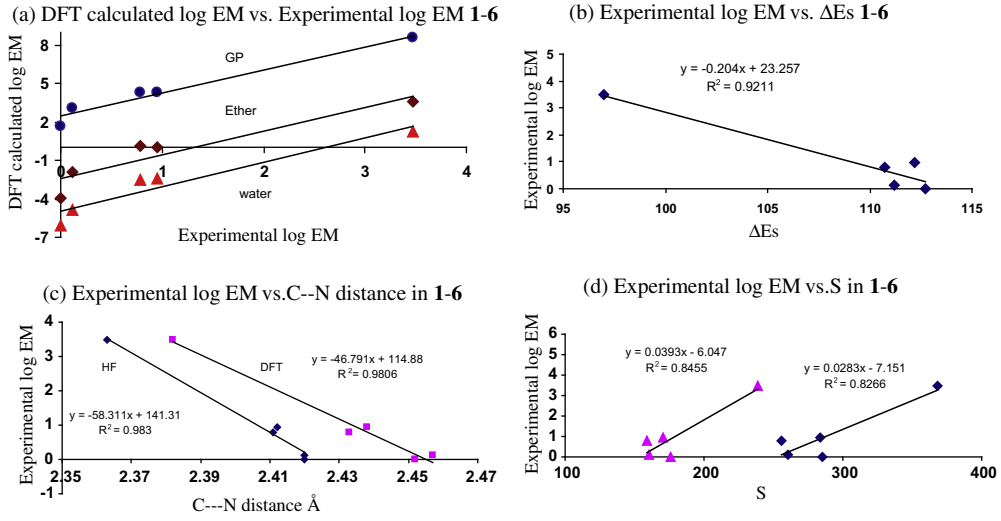


**Fig. 2.** (a) Plot of the calculated DFT in the gas phase (GP), in ether and in water vs. the experimental effective molarity (log EM) in **1**–**6**. (b) Plot of the experimental effective molarity (log EM) vs. MM2 calculated $\Delta E_s$ (P-SM) of the products and reactants in **1**–**6**. (c) Plot of the experimental effective molarity (log EM) vs. the S values for $\Delta H$ vs. $1/r$, curve 1 and $\Delta H$ vs. sin $\alpha$, curve 2 in **1**–**6**. (d) Plot of the experimental effective molarity (log EM) vs. the HF and DFT calculated C–N distance in **1**–**6**.

neighboring negative charge (Chart 3) than that in the corresponding ground state. The magnitude of the charge distribution effect is likely to be much stronger in water than in other less-polar solvents (gas phase or ether). In the case of the intramolecular processes, the effect of the charge distribution is minimized due to the lack of the negative charge in the structures of the ground and transition states. Therefore, it is reasonable to assume that intramolecular processes leading to transition states characterized with charge separation (electrostatic forces) will be more efficient than those lacking the charge distribution effect, especially in those cases where water is the reaction medium. (iii) The substituent effect in intramolecular processes **1**–**6** is largely affected by the nature of the solvent. In the gas phase, the effect is much more pronounced than in water. For example, the difference in the activation energies between the most and the least reactive processes is nearly 5.5 kcal/mol when the intramolecular process calculations are carried out in the gas phase, whereas when the calculations are done in water the calculated value is less than 3 kcal/mol (Table 2). It is tempting to extrapolate these results to biological systems. Accordingly, we propose that the rate of intramolecular process taking place in biological system will vary according to the environment in the active site. The intramolecular rate in polar biological environment will be much lower than that in the less-polar environment. (iv) Although the calculated and the experimental EM values are comparable there is a discrepancy in their absolute values. This is due to the fact that the experimental measurement of the effective molarities was conducted in the presence of 50% dioxan in water as a solvent. This solvent mixture differs in its properties from water and ether (different dielectric constant value) hence it is expected that the experimental absolute effective molarities for processes **1**–**6** will have different values from these calculated in water and ether [17].

It is worth noting that the structure of the intermolecular control in processes 13–15 has a carboxylate present ($ClCH_2C(O)O^-$), which expected to have undue effect on the thermodynamic and kinetic properties of the intermolecular system since a positive charge is built of close by; this feature is not in the corresponding intramolecular structures.

It should be emphasized that attempts to correlate the effective molarity values with the intramolecular activation energy

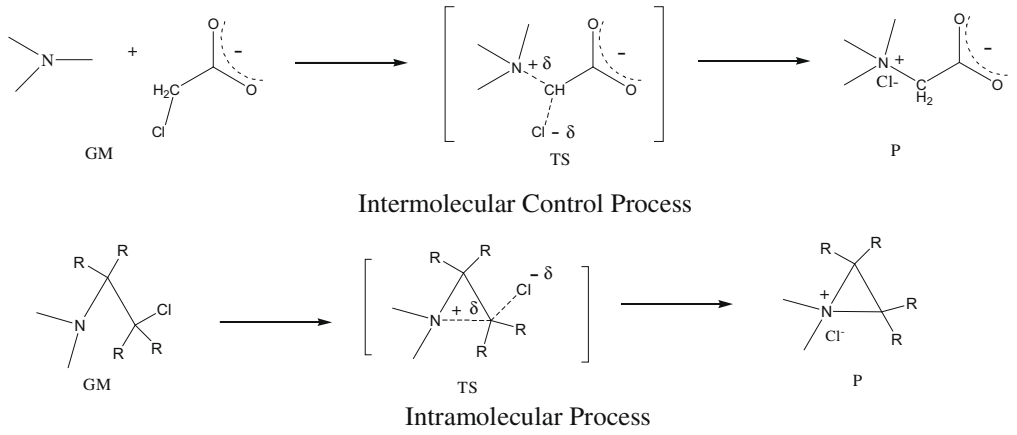


**Chart 3.** Representative examples showing the charge distribution in intermolecular control and intramolecular processes for ring-closing reactions of substituted 3-aminoalkyl halides to aziridines.

($\Delta G^{\ddagger}_{S\ \mathrm{intra}}$) resulted in a random correlations ($R$ less than 0.4). The only strong correlation was obtained when the EM values were plotted against the gas phase $\Delta G^{\ddagger}_{S\ \mathrm{intra}}$ values ($R = 0.98$).

In order to shed light on the nature of the driving forces behind the effect of the substituent on the ring-closing rates of **1**–**6**, the effective molarity values (log EM) were examined for linear correlation with the MM2 strain energy values ($\Delta E_s$) as well as with the calculated distances between the two reactive centers (C2–N1). The correlation results along with their correlation coefficients are summarized in the equations depicted in Fig. 2b and c. The correlation results indicate strong correlation of the EM values with both the C2–N1 distance and the difference in the ground state energies of the products and the reactants ($\Delta E_s$). Derivatives with short C–N distances and low $\Delta E_s$ values undergo ring-closing reactions in higher rates than those having long C–N distances and high $\Delta E_s$ values and vice versa.

To further investigate the mutual relationship between the C–N distance and $\Delta E_s$ we calculated the change in the value of the attack angle $\alpha$ (N1/C2/⟨alpha⟩–C3, Chart 4) and the change in the distance between the two reactive centers ($r$ = N1–C2 distance) as a function of $\Delta H$ (enthalpic energy) since both parameters $r$ and $\alpha$ are reported to play an important role in the reaction rates of intramolecular systems [4,8].

It should be noted that the values of $\Delta H$, $r$ and $\alpha$ were obtained from HF calculations of the energy profiles of the amine nitrogen (N1) approach towards the electrophilic center (C2) in each of the reactants for **1–6** until reaching the transition state. The calculation results of these approaches are summarized in Table S1.

The data of Table S1 ($\Delta H$, sin $\alpha$ and $r$) was examined for linear correlations. Good correlations with high correlation coefficients were obtained from the plot of the enthalpic energy ($\Delta H$) and sin $\alpha$ and $1/r$ ($R = 0.98$–$0.99$). The slope values of the resulting equations are summarized in Table S2. Careful examination of Table S2 indicates that the energy needed to increase the value of angle $\alpha$ to reach the optimal value for the formation of a stable transition state is less for **6** than for **1**. This suggests that it is easier for N1 to approach C2 in system **6** than that in system **1**. Further, when the S values were plotted against log EM values, good correlations were obtained (Fig. 2d). Further, it was found that the $S$ value is largely dependent on the ground state energies of the reactants and products ($\Delta E_s$). Processes with high $\Delta E_s$ values are characterized with low $S$ values and vice versa.

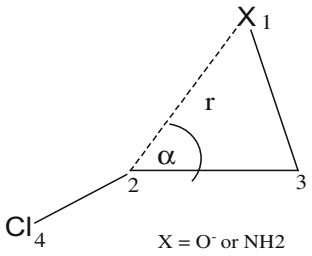


**Chart 4.** Cartoon representation of the attack angle $\alpha$ and the X1–C2 distance, $r$, in the ring-closing reactions of **1**–**12**.

### 3.2. Ring-closing reactions of substituted chlorohydrins

In a similar manner to that for processes **1**–**6**, the calculated EM values for processes **7**–**12** (Table 2) were examined for linear correlations with the experimental effective molarity values. The correlation results summarized in the equation and illustrated in Fig. 3a indicate strong correlation between the two parameters ($R = 0.97$). It should be indicated that the calculated effective

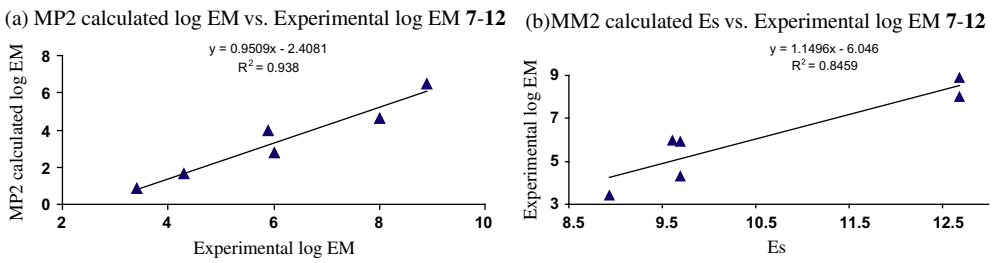


**Fig. 3.** (a) Plot of the calculated MP2 in water vs. the experimental effective molarity (log EM) in **7**–**12**. (b) Plot of the experimental effective molarity (log EM) vs. MM2 calculated $E_s$ of the products in **7**–**12**.

molarities for processes **7**–**12** are underestimated (about $10^2$ M). This is might be due to the fact that the EM measurements were carried out using a mixture of methanol/water as a solvent whereas the calculations were run in the presence of water as a solvent. Despite the underestimation of the calculated absolute values the calculated relative effective molarities are in perfect agreement with the experimental EM values. For example the difference between the higher and the lower EM values as obtained from the MP2 calculations is 5.6 (log EM) whereas the difference in the experimentally determined ones is 5.5 (Table 2).

In addition, when the effective molarity values for processes **7**–**12** were examined for linear correlation with the MM2 strain energies of the products ($E_s$) good correlation with a correlation coefficients ($R$) 0.92 was obtained (Fig. 3b). The correlation results indicate that derivatives yielding strained rings (high $E_s$ values) undergo ring-closing reactions in lower rates than these leading to unstrained rings (low $E_s$ values). This is similar to that found for **1**–**6**.

## 4. Summary and conclusions

The combined results reported in (a) and (b) reveal: (1) the effective molarity (intramolecular activation energy) in the two systems studied herein is dependent on both the angle of attack of the nucleophile ($NH_2$ or $O^-$) on the carbon attached to chlorine and the distance between the nucleophile ($NH_2$ or $O^-$) and the electrophile (C–Cl), (2) systems having small difference in the strain energies of their products and reactants such as system **6** are more reactive than these with large difference, and the reactivity extent is linearly correlated with the strain energy difference ($\Delta E_s$), (3) the energy needed to provide a stable transition state for a strained system is less than that for the unstrained systems due to the similarity in the structures of the reactants and the corresponding products, (4) our results do not contraindicate with Menger's postulation on the critical distance of less than 3 Å (diameter of water) to reach rate enhancements as a result of desolvation of water. Further we believe that desolvation is a form of strain, and our strain theory, in this sense coincides with spatio-temporal effects.

In conclusion, we have derived an equation that can be utilized to predict effective molarities for intramolecular processes that are difficult to be experimentally obtained. Further, we expanded on the equation derived by Menger that relates rate and distance to a new equation that relates both angle of attack and distance. This novel equation combines both hypotheses of Menger and coworkers [4] and Koshland and coworkers [3] and shows that neither distance alone nor angle of attack alone is the dominant factor in rates enhancements in intramolecular reactions. Moreover, we have shown that strain energy is a factor in rate accelerations in some intramolecular reactions but this factor strain is actually a function of distance and angle of attack.

## Acknowledgments

We thank the Karaman Co. and the German–Palestinian–Israeli fund agency for support of our computational facilities. We would also like to give special thanks to Dr. Omar Deeb, Sherin Alfalah, Nardene Karaman, Rowan Karaman and Donia Karaman for computational software support and technical assistance.

## Appendix A. Supplementary data

Xyz Cartesian coordinates for the calculated GM and TS optimized structures in processes **1–16**. Table S1: HF energy profiles for 1–6 ($\Delta H$, $r$ and sin $\alpha$). Table S2: slope values of $\Delta H$ vs. $1/r$ and $\Delta H$ vs. sin $\alpha$. Supplementary data associated with this article can be found, in the online version, at doi:10.1016/j.bioorg.2010.04.002.

## References

[1] For a review in this topic, see A.W. Czarnik, in: J.F. Liebman, A. Greenberg (Eds.), Mechanistic Principles of Enzyme Activity, VCH Publishers., New York, NY, 1988;
T.C. Bruice, S.J. Benkovic, Bioorganic Mechanisms, vols. I and II, Benjamin, Reading, MA, 1966;
W.P. Jencks, Catalysis in Chemistry and Enzymology, McGraw, New York, 1969;
M.L. Bender, Mechanism of Homogeneous Catalysis from Protons to Proteins, Wiley Interscience, New York, 1971;
D.L. Nelson, M.M. Cox, Lehninger Principles of Biochemistry, Worth Publishers, New York, 2003;
A. Fersht, Structure and Mechanism in Protein Science: A guide to Enzyme Catalysis and Protein Folding, W.H. Freeman and Company, New York, 1999;
R. Pascal, Eur. J. Org. Chem. (2003) 1813;
R. Pascal, Bioorg. Chem. 31 (2003) 485;
G.F. Sweigers, Mechanical Catalysis, John Wiley & Sons, Hoboken, NJ, 2008;
C. Walsh, Enzymatic Reaction Mechanism, Freeman, San Francisco, 1979. p. 978;
M.I. Page, in: M.I. Page, A. Williams (Eds.), Enzyme Mechanisms, R. Soc. Chem., London, 1987, p. 1;
R.B. Silverman, The Organic Chemistry of Enzyme-catalyzed Reactions, San Diego Academic, 2002. p. 717;
R. Pascal, Eur. J. Org. Chem. (2003) 1813;
D.A. Kraut, K.S. Carroll, D. Herschlag, Annu. Rev. Biochem. 72 (2003) 517;
A. Radzicka, R. Wolfenden, J. Am. Chem. Soc. 118 (1996) 6105;
M.J. Snider, R. Wolfenden, J. Am. Chem. Soc. 122 (2000) 11507.
[2] T.C. Bruice, F.L. Lightstone, Acc. Chem. Res. 32 (1999) 127;
F.L. Lightstone, T.C. Bruice, J. Am. Chem. Soc. 119 (1997) 9103;
F. L Lightstone, T.C. Bruice, J. Am. Chem. Soc. 118 (1996) 2595;
F.L. Lightstone, T.C. Bruice, J. Am. Chem. Soc. 116 (1994) 10789;
T.C. Bruice, W.C. Bradbury, J. Am. Chem. Soc. 90 (1968) 3803;
T.C. Bruice, W.C. Bradbury, J. Am. Chem. Soc. 87 (1965) 4846;
T.C. Bruice, U.K. Pandit, J. Am. Chem. Soc. 82 (1960) 5858;
T.C. Bruice, U.K. Pandit, Proc. Natl. Acad. Sci. USA 46 (1960) 402.
[3] A. Dafforn, D.E. Koshland Jr., Proc. Natl. Acad. Sci. USA 68 (1971) 2463;
A. Dafforn, D.E. Koshland Jr., Bioorg. Chem. 1 (1971) 129.
[4] F.M. Menger, M. Ladika, J. Org. Chem. 35 (1990) 3006;
F.M. Menger, M. Ladika, J. Am. Chem. Soc. 110 (1988) 6794;
F.M. Menger, Acc. Chem. Res. 18 (1985) 128;
F.M. Menger, J.F. Chow, H. Kaiserman, P.C. Vasquez, J. Am. Chem. Soc. 105 (1983) 4996;
F.M. Menger, Tetrahedron 39 (1983) 1013;
F.M. Menger, J. Grosssman, D.C. Liotta, J. Org. Chem. 48 (1983) 905;
F.M. Menger, A.L. Galloway, D.G. Musaev, Chem. Commun. (2003) 2370;
F.M. Menger, Pure Appl. Chem. 77 (2005) 1873. and references therein.
[5] S. Milstein, L.A. Cohen, J. Am. Chem. Soc. 92 (1970) 4377;
S. Milstein, L.A. Cohen, Proc. Natl. Acad. Sci. USA 67 (1970) 1143;
S. Milstein, L.A. Cohen, J. Am. Chem. Soc. 94 (1972) 9158;
M.I. Page, W.P. Jencks, Proc. Natl. Acad. Sci. USA 68 (1971) 1678;
M.I. Page, W.P. Jencks, Gazz. Chim. Ital. 117 (1987) 455;
M.I. Page, Chem. Soc. Rev. 2 (1973) 295;
M.I. Page, Angew. Chem. Int. Edit. Engl. 16 (1977) 449.
[6] M.I. Page, W.P. Jencks, Proc. Natl. Acad. Sci. USA 68 (1971) 1678;
M.I. Page, W.P. Jencks, Gazz. Chim. Ital. 117 (1987) 455;
M.I. Page, Chem. Soc. Rev. 2 (1973) 295;
M.I. Page, Angew. Chem. Int. Edit. Engl. 16 (1977) 449.
[7] A.J. Kirby, Adv. Phys. Org. Chem. 17 (1980) 183. and references therein.
[8] R. Karaman, Tet. Lett. 49 (2008) 5998;
R. Karaman, Bioorg. Chem. 37 (2009) 11;
R. Karaman, Tet. Lett. 50 (2009) 452;
R. Karaman, Res. Lett. Org. Chem., doi: 10.1155/2009/240253.;
R. Karaman, Bioorg. Chem. 37 (2009) 106;
R. Karaman, J. Mol. Struct. 910 (2009) 27;
R. Karaman, Tet. Lett. 50 (2009) 6083;
R. Karaman, J. Mol. Struct. (Theochem.) 939 (2010) 69;
R. Karaman, Tet. Lett. 50 (2009) 7304;
R. Karaman, J. Mol. Struct. (Theochem.) 940 (2010) 70.
[9] For recent review, see C. Galli, L. Mandolini, Eur. J. Org. Chem. (2000) 3117.
[10] http://w/w/w.gaussian.com.
[11] U. Burker, N.L. Allinger, Molecular Mechanics, American Chemical Society, Washington DC, 1982.
[12] C.J. Casewit, K.S. Colwell, A.K. Rappe', J. Am. Chem. Soc. 114 (1992) 10024;
C.J. Casewit, K.S. Colwell, A.K. Rappe', J. Am. Chem. Soc. 114 (1992) 10035;
C.J. Casewit, K.S. Colwell, A.K. Rappe', J. Am. Chem. Soc. 114 (1992) 10046.
[13] M.J.S. Dewar, E.G. Zoebisch, E.F. Healy, J.J.P. Stewart, J. Am. Chem. Soc. 107 (1985) 3902.
[14] J.N. Murrell, K.J. Laidler, Trans Faraday Soc. 64 (1968) 371.

[15] K. Fukui, Acc. Chem. Res. 14 (1981) 363;
K. Muller, Angew. Chem. Int. Edit. Engl. 19 (1980) 1.
[16] M.T. Cancès, B. Mennucci, J. Tomasi, J. Chem. Phys. 107 (1997) 3032;
B. Mennucci, J. Tomasi, J. Chem. Phys. 106 (1997) 5151;
B. Mennucci, E. Cancès, J. Tomasi, J. Phys. Chem. B 101 (1997) 10506;
J. Tomasi, B. Mennucci, E. Cancès, J. Mol. Struct. (Theochem.) 464 (1999) 211.
[17] It should be noted that DFT calculations in the presence of 50% dioxan in water are not feasible.